

**Abstract**

Recombinant inbred line (RIL) populations of peanut (*Arachis hypogaea* L.) are being used to develop markers for resistance to several diseases, including late leaf spot, caused by *Cercosporidium personatum*. In efforts to develop molecular markers to assist in selection for resistance to late leaf spot, several populations have been developed from parents with varying levels of resistance. Breeding programs are faced with the challenge of phenotyping large numbers of genotypes in a timely manner with a limited number of people. Unmanned aerial systems (UAS) may have potential to help overcome this challenge. Through the use of a UAS, imaging techniques, and ground truthing we developed an analysis method to quickly and easily assess late leaf spot severity in the field. This experiment utilized 79 RILs with varying levels of susceptibility to late leaf spot and seven parental lines. With accurate ground truthing, late leaf spot can be differentiated from other diseases in the field by the necrotic lesions on all above ground plant parts and defoliation. By testing vegetative indices (VIs) in ArcMap (ESRI, Redlands, CA 92373 USA) we could determine the percent change of each VI over the course of the season. This percentage was then used to determine the correlation with visual ratings. Analyses show a positive correlation between the normalized difference vegetation index and final visual ratings with a correlation coefficient of 0.606 (p-value < 0.05). Results suggest that through the use of a UAS equipped with a multispectral camera, the percent change in VIs can be positively correlated to visual ratings. This technique could greatly increase the efficiency of peanut breeding programs.

**Introduction**

Cultivated peanut (*Arachis hypogaea* L.) is susceptible to many diseases including the fungal disease late leaf spot, caused by *Cercosporidium personatum* (Berk. & M. A. Curtis) (3). Late leaf spot symptoms can appear on any above ground parts of the peanut making it easy to be diagnosed visually. However, field screening for resistance to the disease requires a relatively large number of plants, considerable space, and massive amounts of time.

The use of unmanned aerial systems (UASs) in agriculture has increased greatly due to their wide range of uses. In combination with powerful data analysis methods UASs can deliver real-time information of high spatial and temporal resolution in non-destructive ways. Multispectral images have been used to detect plant diseases with varying levels of success in recent years (4). The development of automated methods that rely on multispectral images for analysis could be useful in identifying and rating late leaf spot in a reliable and rapid way. With a lack of research being done in the area in peanut diseases the following objective was created. The objective of this study was to test vegetative indices to develop aerial imaging techniques using a UAS for assessing late leaf spot severity in field evaluations of peanut genotypes and determine the relationship between assessments made with aerial imaging and visual ratings.

**Methods**

**Field Setup**

- A field experiment was conducted at the University of Georgia, Lang Farm, Tifton, GA in 2016.
- Randomized complete block design with three replicates of each genotype.
- Bordered on both sides by the susceptible cultivar TUFRunner 511 (3).

**Selection of Genotypes**

- 64 genotypes with varying levels of resistance to late leaf spot were selected from four mapping populations along with their parental lines. This resulted in 79 genotypes tested (Table 1).



Fig. 1. MicaSense RedEdge multispectral camera mounted on DJI Phantom 2 quadcopter.

**Methods**

Table 1. Recombinant inbred lines selected for comparison.

S Population	T Population	F799 Population	I801 Population
S4	T11	596	917
S17	T17	600	924
S24	T20	602	943
S51	T21	607	946
S75	T22	608	952
S98	T48	626	954
S102	T49	643	971
S119	T70	660	980
S128	T71	663	981
S179	T106	691	982
S197	T113	693	1001
S223	T120	700	1008
S276	T133	704	1012
S316	T142	708	1028
S329	T145	712	1036
S338	T148	713	1040
S344	T158	724	1042
S347	T219	757	1075
SunOleic 97R	GT-C20	Tifrunner	SPT 06-06
NC94022	Tifrunner	NC3033	Florida-07

**Visual Data Collection**

- The Florida 1 to 10 scale was used to rate disease severity as described by Chiteka, et al. (1).
- Ratings were taken at 90, 104, 113, 121, and 135 DAP.

**Aerial Data Collection**

- Multispectral images of the field were collected with a MicaSense RedEdge multispectral camera mounted on a DJI Phantom 2 quadcopter (Fig. 1).
- The MicaSense Rededge camera collects five spectral bands: blue (480 nm), green (560 nm), red (670 nm), red edge (720 nm), and near infrared (840 nm).

**Image Processing**

- Images were uploaded to the MicaSense ATLAS data processing system to be aligned and stitched into a GEOTIFF image (Fig. 4).
- Images were further processed using ArcMap 10.4.1 (ESRI, Redlands, CA 92373 USA) as seen in Fig. 3.

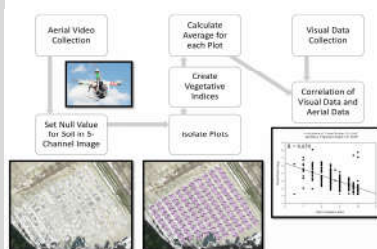


Fig. 3. Image processing for aerial analysis of late leaf spot.

**Statistical Analysis**

- Pearson's correlation coefficients were to gage correlations between aerial and visual ratings using SigmaPlot 13.0.

**Results**

Table 2. Vegetative Indices, their formula, and the corresponding Pearson's correlation coefficient (R) for visual versus aerial ratings at each rating date.

Vegetative Index <sup>a</sup>	Formula <sup>a</sup>	Visual Rating <sup>a</sup> 83 DAP		Visual Rating <sup>a</sup> 121 DAP	
		R	R	R	R
Ratio VI	NIR-RE	0.323	0.496	0.597	0.537
Normalized Red	R/(NIR-RE+G)	0.303	0.400	0.600	0.527
Normalized Red - Farth RE	R/(NIR-RE+G)	0.295	0.402	0.597	0.527
Normalized Difference VI	(NIR-R)/(NIR+R)	0.302	0.370	0.583	0.522
Optimized Soil Adjusted VI	(NIR-R)/(NIR+R+16)	0.302	0.370	0.583	0.522
Difference VI	NIR-G	0.397	0.511	0.606	0.519
Green Difference VI	NIR-G	0.398	0.523	0.584	0.457
Normalized Near Infrared	NIR/(NIR+G)	0.324	0.523	0.578	0.505
Normalized Pigment - RE	(RE-B)/(RE+B)	0.241	0.316	0.584	0.479
Normalized Excess Blue	(L*BI-G)/(L*BI+G)	0.217	0.301	0.603	0.461
Green VI - RE	NIR-G	0.412	0.505	0.569	0.425
Green Ratio VI	(G)/(NIR+RE+G)	0.307	0.499	0.541	0.382
Green Normalized Difference VI	(NIR-G)/(NIR+G)	0.318	0.472	0.528	0.364
Normalized NIR - RE	(NIR-RE)/(NIR+RE+G)	0.337	0.498	0.533	0.340
Excess Red - RE	L*BI-RE	0.237	0.330	0.444	0.336
Normalized Difference VI - RE	(NIR-RE)/(NIR+RE)	0.347	0.499	0.521	0.284
Ratio VI - RE	NIR-RE	0.337	0.462	0.520	0.283

<sup>a</sup>VI = Vegetation Index, RE = Red edge band replaces red band.  
<sup>b</sup>B = Blue band (480 nm), G = Green band (560 nm), R = Red band (670 nm), NIR = Near infrared band (670 nm), RE = Red edge band (720 nm).

Table 3. Vegetative Indices, their formula, and the corresponding Pearson's correlation coefficient (R) for visual rating versus percent change in aerial rating at each rating date.

Vegetative Index <sup>a</sup>	Formula <sup>a</sup>	Visual Rating <sup>a</sup> 83 DAP		Visual Rating <sup>a</sup> 121 DAP	
		Percent Change <sup>b</sup>	R	Percent Change <sup>b</sup>	R
Normalized Near Infrared	NIR/(NIR+R+G)	0.606	0.487		
Normalized Excess Blue	(L*BI-G)/(L*BI+G)	0.605	0.435		
Normalized Difference VI	(NIR-R)/(NIR+R)	0.600	0.524		
Optimized Soil Adjusted VI	(NIR-R)/(NIR+R+16)	0.600	0.524		
Normalized Pigment - RE	(RE-B)/(RE+B)	0.561	0.435		
Normalized Difference VI	(NIR-G)/(NIR+G)	0.551	0.343		
Normalized Red - RE	R/(NIR+RE+G)	0.542	0.390		
Difference VI	NIR-G	0.534	0.432		
Ratio VI	NIR-R	0.532	0.321		
Normalized Red	R/(NIR+R+G)	0.499	0.323		
Normalized Green - RE	G/(NIR+RE+G)	0.496	0.251		
Normalized Difference VI - RE	(NIR-RE)/(NIR+RE)	0.477	0.190		
Green Ratio VI	NIR-G	0.475	0.213		
Normalized NIR - RE	NIR/(NIR+RE+G)	0.470	0.200		
Green VI - RE	(G)/(NIR+RE)	0.453	0.304		
Green Difference VI	NIR-G	0.440	0.282		
Difference VI - RE	NIR-RE	0.437	0.239		
Ratio VI - RE	NIR-RE	0.282	0.0301		
Excess Red - RE	L*BI-RE	0.208	0.223		
Normalized Red - RE	RE/(NIR+RE+G)	0.110	0.0770		

<sup>a</sup>Ratings for late leaf spot (*Cercosporidium personatum* (Berk. & M. A. Curtis)) were taken based on the Florida 1-10 scale (1).  
<sup>b</sup>Percent change was calculated by subtracting the later rating from the initial rating and dividing by the initial rating and then multiplying by 100.  
<sup>c</sup>VI = Vegetation Index, RE = Red edge band replaces red band.  
<sup>d</sup>B = Blue band (480 nm), G = Green band (560 nm), R = Red band (670 nm), NIR = Near infrared band (670 nm), RE = Red edge band (720 nm).

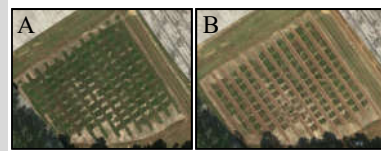


Fig. 4. GEOTIFF images collected from MicaSense ATLAS data processing system at A) 121 DAP and B) 135 DAP.

**Results**

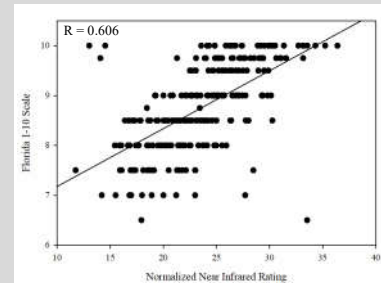


Fig. 5. Pearson's correlations between percent change from 83 to 121 DAP and normalized near infrared rating from 121 DAP (p < 0.001).

**Conclusions**

- Vegetative indices can be positively correlated to late leaf spot ratings and the ratio vegetative index had the strongest correlation with late leaf spot ratings using the Florida 1-10 scale (Table 2).
- Stronger correlations can be achieved in some vegetative indices by utilizing percent change of the severity of the disease over the season (Table 3).
- The strongest correlations were made when using the percent change in aerial ratings taken at 83 DAP and 121 DAP with visual ratings at 121 DAP with the normalized near infrared VI (Fig. 3).
- There are three main advantages to using aerial imagery: images collected are permanent, rating time is greatly reduced, and images can be standardized.
- Results suggest that through the use of a UAS equipped with a multispectral camera aerial ratings could greatly increase the efficiency of peanut breeding programs.

**References**

- Chiteka, Z. A., Gorbet, D. W., Shokes, F. W., Kucharek, T. A., and Knauff, D. A. 1988. Components of Resistance to Late Leafspot in Peanut. I. Levels and Variability - Implications for Selection. *Peanut Sci.* 15:25-30.
- Smith, D. H. and Littrell, R. H. 1980. Management of peanut foliar diseases. *Plant Dis.* 64:356-361.
- Tillman, B., M. Gomillion, J. McKinney, and G. Person. 2015. Peanut Variety Performance in Florida, 2011-2014. University of Florida. Assessed on March 18, 2017.
- Zhang, C., and Kovacs, J. M. 2012. The application of small unmanned aerial systems for precision agriculture: a review. *Precis. Agric.* 13:693-712.